

Tell Me What to Track: Infusing Robust Language Guidance for Enhanced Referring Multi-Object Tracking

Wenjun Huang¹, Yang Ni¹, Hanning Chen¹, Yirui He¹, Ian Bryant¹, Yezi Liu¹, Mohsen Imani¹

¹ University of California, Irvine, CA, USA

{m.imani}@uci.edu

Abstract

Referring multi-object tracking (RMOT) is an emerging autonomous driving task that aims to localize an arbitrary number of targets based on a language expression and continuously track them in a video. This intricate task involves reasoning on multi-modal data and precise target localization with temporal association. However, prior studies overlook the imbalanced data distribution between newborn targets and existing targets due to the nature of the task. In addition, they only indirectly fuse multi-modal features, struggling to deliver clear guidance on newborn target detection. To solve the above issues, we conduct a collaborative matching strategy to alleviate the impact of the imbalance, boosting the ability to detect newborn targets while maintaining tracking performance. In the encoder, we integrate and enhance the cross-modal and multi-scale fusion, overcoming the bottlenecks in previous work, where limited multi-modal information is shared and interacted between feature maps. In the decoder, we also develop a referring-infused adaptation that provides explicit referring guidance through the query tokens. The experiments on the according autonomous driving datasets showcase the superior performance of TellTrack (+3.42%) compared to prior works, demonstrating the effectiveness of our designs.

1. Introduction

Over the past decades, multi-object tracking (MOT) has played an important role in autonomous driving [26], where understanding and monitoring the movement of multiple entities over time is critical. MOT can be defined as the process of following the trajectories of a set of objects

This work was supported in part by the DARPA Young Faculty Award, the National Science Foundation (NSF) under Grants #2127780, #2319198, #2321840, #2312517, and #2235472, the Semiconductor Research Corporation (SRC), the Office of Naval Research through the Young Investigator Program Award, and Grants #N00014-21-1-2225 and #N00014-22-1-2067, and Army Research Office Grant #W911NF2410360. Additionally, support was provided by the Air Force Office of Scientific Research under Award #FA9550-22-1-0253, along with generous gifts from Xilinx and Cisco.

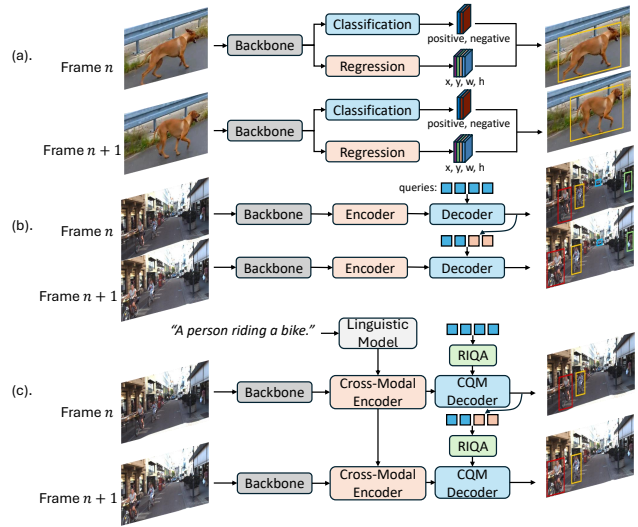


Figure 1. Tracking pipelines for SOT, MOT, and our proposed pipeline for RMOT. (a). SOT focuses on tracking one object and maintaining its location with a classification head and a regression head. (b). MOT tracks multiple objects simultaneously and manages multiple identities. (c). We propose a framework for RMOT that considers the language prompt (“A person riding a bike.” in this case) and only tracks the targets meeting the description. The proposed framework consists of a novel referring-infused query adaptation (RIQA) module, a collaborative query matching (CQM) decoder, and a cross-modal encoder (CME).

through different frames while keeping their identities discriminated. Compared with single object tracking (SOT) [3, 4, 16], MOT not only detects and associates more objects but also manages unique identities for each object and handles frequent occlusions.

Traditional MOT methods often lack the nuanced understanding required to follow specific targets when guided by natural language descriptions, a challenge that becomes particularly evident when users wish to focus on objects of interest described semantically. Meanwhile, referring understanding [12, 18, 35, 42] that integrates natural language processing into scene perception has raised great attention, with the advancement of vision-language models (VLMs).

It aims to localize targets of interest in images or videos under the instruction of human language. In this paper, we focus on an emerging task named referring multi-object tracking (RMOT), which enhances conventional MOT and takes into account language understanding. RMOT improves MOT’s ability to meet human intentions, significantly broadens the applicability, and boosts functional efficiency. Instead of tracking all visible objects in the scene, RMOT aims at tracking only the referent targets. For example, if we input “A person riding a bike” as the text prompt, the tracker should only track the ones meeting the description while ignoring other objects such as “cars” and “a person on foot”, which are also tracked in MOT. Fig. 1 illustrates the typical tracking pipelines for SOT, MOT, and our proposed pipeline for RMOT.

Nevertheless, current transformer-based models are faced with several challenges that lead to a sub-optimal performance in RMOT [35, 47]. First of all, based on the transformer architecture, they train a joint decoder for newborn target detection and existing target tracking. However, the imbalanced distribution of newborn targets and existing targets in the dataset impairs the training of newborn target detection. While the query tokens for existing targets, referred to as “track queries” are activated and trained during the whole lifespan of the targets, the queries for newborn targets, referred to as “detection queries”, are only activated once when the targets first appear in the video. This insufficient training in newborn target detection leads to poor performance when dealing with uncommon targets.

In terms of language guidance, current designs fuse the text embedding with image features right after the vision backbone, providing a mixed-modal feature map to later stages. However, the fused feature is not a direct input to the most critical decoder and contains no explicit semantic information, leading to relatively weak and indirect language guidance that cannot be effectively reasoned in the decoder. Recent work, such as Segment Anything (SAM) [19, 31], adopts a different paradigm to fuse images and prompts. Specifically, SAM concatenates the prompt embedding and query tokens as the input to the decoder, providing strong and direct guidance. However, models like SAM cannot be naively applied in RMOT. Despite its strong zero-shot segmentation performance, SAM requires explicit point or box prompts to focus on a specific instance and does not support arbitrary language guidance or newborn target detection, not fitting the need of the RMOT task.

Observing the aforementioned challenges, we propose a new RMOT algorithm, named “Tell Me What to Track” (TellTrack). On one hand, TellTrack propose a strategy that relaxes the matching criteria and thereby increases the activation frequency of the detection queries. During training, the existing targets are not solely matched with track queries but also can be matched with detection queries. On the other

hand, TellTrack adopts a query adaptor that directly fuses the text prompt with the queries, providing strong guidance and enhancing the model’s reasoning capability. Before the decoder, TellTrack also develops a unified encoder that generates a well-rounded fusion of both modalities and effectively incorporates interaction among multi-scale feature maps and text inputs. The key contributions of this work are outlined as follows:

- TellTrack introduce an effective training strategy to boost the model’s detection performance by jointly training the detection queries and track queries, which alleviates the impact caused by the imbalanced distribution of targets.
- Prior works leverage a limited architecture to enable referring in MOT tasks, leading to weak multi-modal fusion and difficulties in understanding nuanced user intention. In contrast, TellTrack provides stronger and more direct guidance to ensure more accurate tracking.
- TellTrack redesign the decoder’s architecture to better integrate the text prompt into the decoder queries; outside of the decoder, we develop a new cross-modal encoder that boosts the information exchange between the multi-modal and multi-scale features.
- Extensive experiments confirm the superior performance of TellTrack, leading to a +3.42% improvement.

2. Preliminaries

Taking the video stream and a language query as inputs, the goal of an RMOT model is to output the track boxes of the corresponding query. A plain transformer-based RMOT model [35], building on top of Deformable DETR [48] and MOTR [43], consists of four key components: feature extractor, encoder, decoder, and temporal reasoning module.

The feature extractor first produces visual and linguistic features for the raw video and text. Given a N -frame video, an image backbone extracts the frame-wise feature pyramid $\mathbf{I}_n^l \in \mathbb{R}^{C_l \times H_l \times W_l}$, where n represents the frame index, and C_l, H_l, W_l represents the channel depth, height, width of the l^{th} level feature map, respectively. At the same time, a linguistic model embeds the text description T into a set of word embeddings $\mathbf{S}_w \in \mathbb{R}^{L \times D}$, where D is the embedding dimension, and L is the number of embedded tokens. Then, an encoder fuses the features of two modalities per frame and gets a stack of vision-language fused embeddings $E_n = \{E_n^1, \dots, E_n^l\}$. For each level of feature maps:

$$E_n^l = \text{Attn}(Q = \text{PE}^I(\mathbf{I}_n^l), K = \text{PE}^S(\mathbf{S}_w), V = \mathbf{S}_w) \quad (1)$$

, where $\text{PE}^I(\cdot), \text{PE}^S(\cdot)$ integrate the positional embeddings into image features and text features, respectively. “Attn” refers to a few attention blocks. A deformable attention encoder [48] is then adopted to further refine the embeddings.

$$E_n' = \text{MSDeformAttn}(E_n, p_q, E_n) \quad (2)$$

, where “MSDeformAttn” follows the notation in [48], and p_q denotes the reference points for deformable attention.

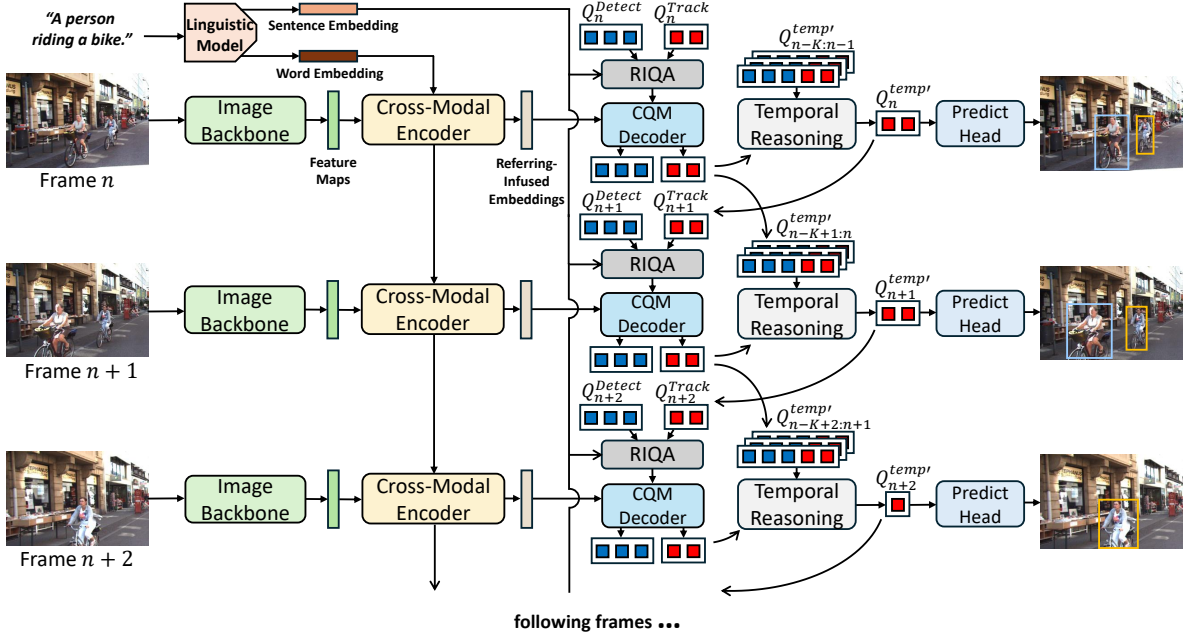


Figure 2. An overview of TellTrack. The transformer-based framework with a memory bank accepts a video frame, a language expression, and a set of learnable queries as input. With the temporal information from past frames in the memory bank, it outputs embeddings corresponding to the tracked targets. RIQA fuses the language information with queries and CQM jointly optimizes the newborn target detection and existing target tracking.

Next, a decoder is used to process a set of learnable queries $Q_n = \{Q_n^{Det}, Q_n^{Tra}\}$ for object detection and tracking. Q_n are categorized into two types: Q_n^{Det} detects potential newborn targets in the current frame, and Q_n^{Tra} represents the tracked targets from the previous frames that aim to locate the same target in the current frame. After self-attending to other queries and cross-attending to the multi-modal embeddings E_n' , the updated queries $Q_n' = \{Q_n^{Det'}, Q_n^{Tra'}\}$ are fed into a referent head (RH) for newborn target detection and existing target tracking. The RH consists of three branches: class, box, and referring. The class branch uses a linear projection to output a binary probability ($\{\hat{c}_n^{Det}, \hat{c}_n^{Tra}\}$), indicating whether the resulting embedding represents a real object. The box branch is a 3-layer feed-forward network (FFN) with ReLU activations, except for the final layer, and predicts the bounding box location ($\{\hat{b}_n^{Det}, \hat{b}_n^{Tra}\}$) for all visible objects. The referring branch is another linear projection that outputs referent scores ($\{\hat{r}_n^{Det}, \hat{r}_n^{Tra}\}$) as binary values, reflecting the likelihood that the object matches the given expression.

After decoding the queries from single-frame features, the temporal reasoning module integrates the information from past frames, in order to refine the boxes and queries. It can be formulated as follows:

$$Q_n^{temp} = \text{Attn}(Q = \text{PE}^T(Q_n'), K = \text{PE}^T(Q_{n-K:n-1}^{temp}), V = Q_{n-K:n-1}^{temp}) \quad (3)$$

$$Q_n^{temp'} = \text{Attn}(Q = \text{PE}^Q(Q_n^{temp}), K = \text{PE}^Q(Q_{n-K:n-1}^{temp}), V = Q_n^{temp}) \quad (4)$$

, where $Q_{n-K:n-1}^{temp}$ are the refined temporal queries of previous K frames; PE^T, PE^Q represent temporal positional encoding, and query positional embedding, respectively. $Q_n^{temp'}$ is the temporal refined queries of the current frame.

Given the temporal refined queries, we calculate the offsets to refine the boxes and get the final predictions $\{\hat{b}_n^{Det'}, \hat{b}_n^{Tra'}\}$.

$$\Delta \hat{b}_n^{Det}, \Delta \hat{b}_n^{Tra} = \text{FFN}(Q_n^{temp'}) \quad (5)$$

$$\hat{b}_n^{Det'}, \hat{b}_n^{Tra'} = \Delta \hat{b}_n^{Det} + \hat{b}_n^{Det}, \Delta \hat{b}_n^{Tra} + \hat{b}_n^{Tra} \quad (6)$$

3. Method

In this section, we elaborate on each newly proposed component in TellTrack, which can readily enhance the performance with a negligible computation overhead: **(1). Collaborative Query Matching (CQM)**. The imbalance of newborn targets and existing targets impairs the overall model performance. We use CQM to facilitate newborn object detection while maintaining the performance of existing target tracking. **(2). Referring-Infused Query Adaptation (RIQA)**. In addition to the indirect fusion of the language

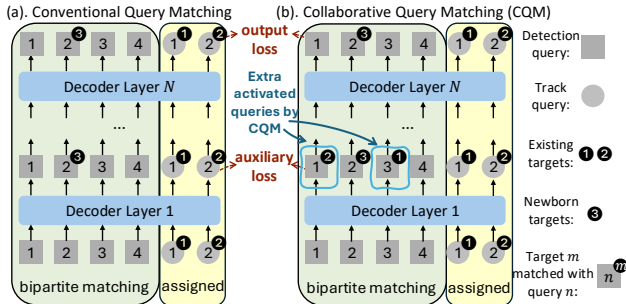


Figure 3. Comparison of conventional query matching and CQM. In both matching, track queries match the pre-assigned existing targets at each decoder layer. Conventional matching performs bipartite matching between detection queries and newborn targets at each layer. In contrast, CQM matches detection queries with both existing and newborn targets in the intermediate decoder layers, except in the final layer. Both methods compute the output loss similarly. However, in CQM, existing targets are also included in the *detection loss* during auxiliary loss calculation (See Sec. 3.4).

description and image in the encoder, we inject a direct information change between the reference and the queries in the decoder, which explicitly guides the queries to detect desired targets. (3). **Cross-Modal Encoder (CME)**. The encoder of previous work suffers from the limited perceptible field of the image features. We develop a new CME to boost the multi-modal fusion by facilitating the information exchange between the multi-scale feature maps and the text. The overview of our method is illustrated in Fig. 2.

3.1. Collaborative Query Matching

Traditional transformer-based MOT algorithms adopt one-to-one bipartite matching for detection queries in all decoder layers. However, the algorithms underestimate the imbalanced activations between detection queries and track queries caused by the natural difference in the number of newborn targets and existing targets in the dataset. That is, any object newly shown up will become existing targets in later frames, making newborn targets relatively sparse in the dataset. Once the target is detected, it is assigned to a track query in the following frames, therefore, each target only activates the detection query once but activates the track query multiple times in the subsequent frames. The insufficient training of detection queries significantly impairs the model performance. To resolve the interference in newborn detection caused by track queries, we propose CQM.

In current auxiliary training, as the example depicted in Fig. 3, the intermediate outputs of each decoder layer are also treated as final outputs and contribute to the loss. In each layer, track queries (1 and 2) are trained to localize the same pre-matched targets (1 and 2), and detection queries do a one-to-one bipartite matching with those newborn targets (3). Therefore, in this example, only one detection query (2) is effectively activated and trained.

Instead of urging a one-to-one matching, CQM allows

the detection queries to match the existing targets in the intermediate layers, as shown in Fig. 3. Except for the final output, the existing targets can be discovered by another detection query besides the assigned track query. In the example, 1 and 2 are not only matched with 1 and 2, respectively, but also are matched with detection queries 3 and 1. Therefore, in addition to 2 is trained by matching with 3, 1 and 3 are also activated. Compared with traditional auxiliary training, CQM significantly boosts the training frequency of detection queries and, as a consequence, improves the model performance.

3.2. Referring-Infused Query Adaptation

Recent works [35, 47] focus on fusing the text prompt with image features in the early stages of the system, which lacks direct guidance for object detection in the later decoder stage. To tackle this, we encode the user semantic intention directly into the queries to provide explicit guidance. The organization of our queries, which follows previous work [24, 29, 34, 48], consists of two parts: *position part*, and *content part*. The position part presents the spatial prior, and the content part represents the semantic prior of the query. Each query has a dimension of $\mathbb{R}^{1 \times 2D}$. The first half of each query is the position part and the second half of each is the content part. Inspired by the decoder architectures of Deformable-DETR [48] and SAM [19], we propose two different types of RIQAs, i.e., pre-decoder adaptation and in-decoder adaptation, that inject sentence embedding into the *content part* of each query. Both the pre-decoder adaptation and the in-decoder adaptation first generate a sentence embedding $\mathbf{S}_s \in \mathbb{R}^{1 \times D}$ of the text prompt T via a frozen sentence encoder and a trainable FFN.

$$\mathbf{S}_s = \text{FFN}(\text{SentenceEncoder}(T)) \quad (7)$$

For infusing referring text, we especially choose sentence embedding over individual word embeddings to provide more general, flexible, and meanwhile less restricted guidance in the query.

3.2.1. Pre-Decoder Adaptation

The overview of pre-decoder adaptation is depicted in Fig. 4 (a). It first fuses linguistic intention with the queries, then feeds the referring-infused queries into the decoder, the same as in previous work. Formally, element-wise \mathbf{S}_s is added to the content part of each query from the last frame $Q_{n-1}[\text{content}]$.

$$Q_{n-1}[\text{content}] = Q_{n-1}[\text{content}] \oplus \mathbf{S}_s \quad (8)$$

, where \oplus represents element-wise addition. The referring-infused queries for the current frame Q_n are obtained

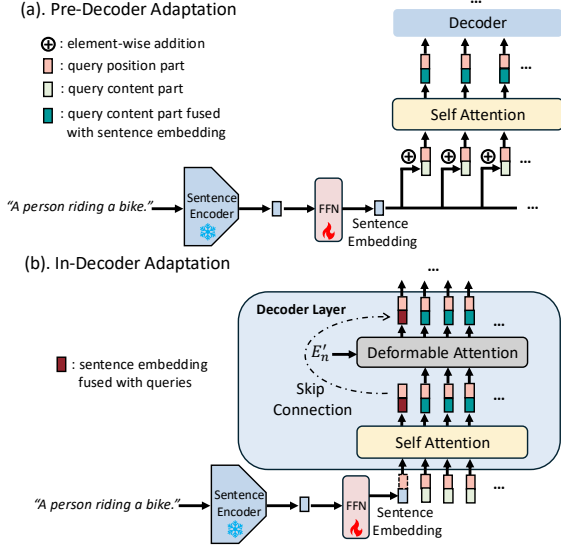


Figure 4. Overview of Referring-Infused Query Adaptation: (a) Pre-Decoder Adaptation and (b) In-Decoder Adaptation. Pre-decoder adaptation integrates sentence embeddings with queries before entering the decoder with an extra self-attention layer. In-decoder adaptation integrates them within the decoder by leveraging the existing self-attention stage. Notice that the sentence embeddings in (b) only participate in self-attention, bypassing the deformable attention between queries and cross-modal features.

through a self-attention layer outside the decoder.

$$\begin{aligned} Q_n &= \text{Attn}(Q = \text{PE}^T(Q_{n-1}), \\ &K = \text{PE}^T(Q_{n-1}), \\ &V = Q_{n-1}) \end{aligned} \quad (9)$$

3.2.2. In-Decoder Adaptation

The in-decoder adaptation uses a different way to fuse linguistic intention with queries, as depicted in Fig. 4 (b). The sentence embedding \mathbf{S}_s first passes through a FFN and then is concatenated with a trainable position part $q_p \in \mathbb{R}^{1 \times D}$ to form a referring query $S'_s \in \mathbb{R}^{1 \times 2D}$. Next, we concatenate this extra query with the original detection and track queries to form a new set of queries $Q_{n_{adapt}} = \{S'_s, Q_n\}$ for in-decoder adaptation, inspired by [17]. Taking the concatenated queries $Q_{n_{adapt}}^{j-1}$, each decoder layer j computes the outputs as follows. We first fuse the information across the queries via self-attention.

$$\begin{aligned} Q_{n_{adapt}}^{j'} &= \text{Attn}(Q = \text{PE}^Q(Q_{n_{adapt}}^{j-1}), \\ &K = \text{PE}^Q(Q_{n_{adapt}}^{j-1}), \\ &V = Q_{n_{adapt}}^{j-1}) \end{aligned} \quad (10)$$

It can be decoupled into two parts $Q_{n_{adapt}}^{j'} = \{S_{s'}^{j'}, Q_{n'}^{j'}\}$. Since the deformable attention has a constraint on the number between the reference points and the queries [48], we

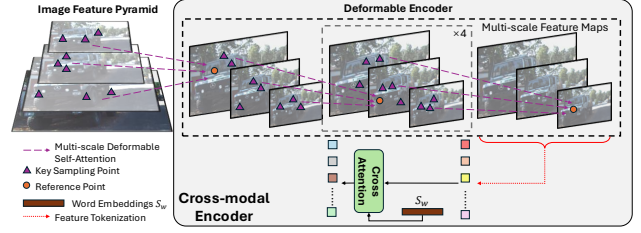


Figure 5. Overview of Cross-modal Encoder (CME). The image feature pyramid is processed by deformable self-attention layers to capture spatial dependencies with key sampling and reference points. The CME then aligns visual and textual information through cross-attention mechanisms, enabling enhanced feature representation learning from word embeddings \mathbf{S}_w .

only do deformable attention between the language fused embeddings E'_n and the non-linguistic queries, i.e., $Q_{n'}^{j'}$.

$$Q_{n_{deform}}^{j'} = \text{MSDeformAttn}(Q_{n'}^{j'}, p_q, E'_n) \quad (11)$$

The output queries of the decoder layer j are obtained by concatenating S'_s with $Q_{n_{deform}}^{j'}$ and forwarding to an FFN with a residual connection.

$$Q_{n_{adapt}}^j = \text{FFN}(\text{Concat}(S'_s, Q_{n_{deform}}^{j'}) + Q_{n_{adapt}}^j) \quad (12)$$

3.3. Cross-Modal Encoder

As introduced in Sec. 2, previous encoder is constructed by a multi-modal fuser (Eq. (1)) followed by a deformable encoder (Eq. (2)). However, this is suboptimal because the raw image feature pyramid at this stage is unstructured, noisy, and lacks hierarchical organization [9, 14]. Since convolutional or transformer-based feature extractors generate dense feature pyramid with redundant and low-level details, and on the other hand, textual representations (\mathbf{S}_w) tend to be abstract and global, direct cross-attention between two modalities may struggle to establish meaningful correspondences, making the alignment process inefficient. As a result, the cross-attention mechanism may focus on irrelevant regions or spread attention too broadly, leading to weak feature fusion and poor multimodal understanding.

Conversely, applying deformable attention on the feature pyramid first enhances the multi-scale spatial structure of visual features before integrating textual information. Deformable attention selectively attends to the most relevant regions across different scales, improving efficiency and reducing redundancy in feature extraction [48]. By refining visual representations beforehand, the model provides a structured, semantically enriched foundation for cross-attention with text. This ensures the text interacts with meaningful, well-organized visual features rather than raw, noisy data. Consequently, the cross-modal alignment process becomes more effective, leading to better fusion of textual and visual information. Therefore, we propose CME,

which can be formally defined as follows:

$$I'_n = \text{MSDeformAttn}(I_n, p_q, I_n) \quad (13)$$

$$E'_n = \text{Attn}(Q = \text{PE}^I(I'_n), K = \text{PE}^S(\mathbf{S}_w), V = \mathbf{S}_w) \quad (14)$$

, and $E'_n = \{E'_n{}^1, \dots, E'_n{}^l\}$. Here, p_q are a set of reference points uniformly distributed on the feature pyramid. As depicted in Fig. 5, each reference point \bullet only attends to a small set of key sampling points \blacktriangle around it across the multi-scale, regardless of the spatial size. The selection of key sampling points is learned via a MLP.

3.4. Loss Function

The loss function can be decoupled as a spatial loss \mathcal{L}^S and a spatial-temporal loss \mathcal{L}^{Temp} . \mathcal{L}^S can be further decoupled as a *track loss* \mathcal{L}^T for existing targets and *detect loss* \mathcal{L}^D for newborn targets. \mathcal{L}^T is obtained via one-to-one computation between the tracking prediction triplet $\hat{y}_n^{Tra} = \{\hat{c}_n^{Tra}, \hat{b}_n^{Tra}, \hat{r}_n^{Tra}\}$ and the groundtruth $y_n^{Tra} = \{c_n^{Tra}, b_n^{Tra}, r_n^{Tra}\}$:

$$\mathcal{L}^T = \lambda_{cls} \mathcal{L}_{cls}(\hat{c}_n^{Tra}, c_n^{Tra}) + \mathcal{L}_{box}(\hat{b}_n^{Tra}, b_n^{Tra}) + \lambda_{ref} \mathcal{L}_{ref}(\hat{r}_n^{Tra}, r_n^{Tra}) \quad (15)$$

, where $\mathcal{L}_{box} = \lambda_{L_1} \mathcal{L}_1 + \lambda_{giou} \mathcal{L}_{giou}$ [32], \mathcal{L}_{cls} and \mathcal{L}_{ref} are focal loss [22]. For \mathcal{L}^D , we find a bipartite graph matching, which of the predicted objects fits the true new-born objects. Given the detection triplet $\hat{y}_n^{Det} = \{\hat{c}_n^{Det}, \hat{b}_n^{Det}, \hat{r}_n^{Det}\}$ and the groundtruth $y_n^{Det} = \{c_n^{Det}, b_n^{Det}, r_n^{Det}\}$, we search for a permutation δ by minimizing matching cost:

$$\hat{\delta} = \arg \min_{\delta} \mathcal{L}_{match}(\hat{y}_n^{Det}, y_n^{Det}(\delta)) \quad (16)$$

, where $\mathcal{L}_{match} = \mathcal{L}_{box} + \lambda_{cls} \mathcal{L}_{cls}$. After determining $\hat{\delta}$, we use it as the new index of the predictions $y_n^{Det}(\hat{\delta})$ to compute \mathcal{L}^D :

$$\mathcal{L}^D = \lambda_{cls} \mathcal{L}_{cls} + \mathbb{I} \lambda_{cls} \mathcal{L}_{cls} + \mathbb{I} \mathcal{L}_{box} \quad (17)$$

, where \mathbb{I} refers to $\mathbb{I}_{\{c^{Det} \neq \emptyset\}}$. In addition, we include auxiliary decoding loss \mathcal{L}_{aux} [1, 9], which calculates \mathcal{L}^T and \mathcal{L}^D using the intermediate outputs, after each decoder layer. When adopting CQM, the $\hat{\delta}_{aux} = \arg \min_{\delta} (\hat{y}_{n,aux_i}^{Det}, [y_n^{Tra}, y_n^{Det}](\delta))$ for the auxiliary losses, where \hat{y}_{n,aux_i}^{Det} denotes the detection triplet of the i -th decoder layer (See Fig. 3). \mathcal{L}^{Temp} , on the other hand, refines the bounding boxes using $\{\hat{b}_n^{Det'}, \hat{b}_n^{Tra'}\}$:

$$\mathcal{L}^{Temp} = \mathcal{L}_{box}(\hat{b}_n^{Tra'}, b_n^{Tra}) + \mathcal{L}_{box}(\hat{b}_n^{Det'}, b_n^{Det}) \quad (18)$$

The final loss is:

$$\mathcal{L} = \mathcal{L}^D + \mathcal{L}^T + \mathcal{L}^{Temp} + \sum_{i=0}^{N_{aux}} \mathcal{L}_{aux_i} \quad (19)$$

, where N_{aux} is the number of decoder layers.

4. Experiments

4.1. Experimental Setup

Datasets. We evaluate the proposed method on two datasets: Refer-KITTI [35] and Refer-KITTI-V2 [47].

Evaluation Metrics. To ensure fair comparison with prior baseline [35], we also employ Higher Order Tracking Accuracy (HOTA) [25] as the primary evaluation metric. HOTA measures the alignment between the predicted and ground-truth trajectories. It provides a comprehensive and balanced assessment by jointly considering the performance of detection and association. It is defined as the geometric mean of detection accuracy (DetA) and association accuracy (AssA), i.e., $HOTA = \sqrt{\text{DetA} \cdot \text{AssA}}$. Additionally, we adopt the following sub-metrics: detection recall/precision (DetRe/DetPr), association recall/precision (AssRe/AssPr), and localization accuracy score (LocA).

Model Details. We leverage the same backbone and text encoder as [35] to extract both image embeddings and linguistic embeddings. As with deformable DETR [48], we adopt the last four feature maps of the backbone as the input to the CME. The parameters associated with the CME are initialized with random values, and the parameters of the text encoder are frozen during training. The remaining parameters are initialized with official pre-trained weights from [48] on the COCO dataset [21]. Our optimization employs AdamW with a base learning rate of 10^{-4} , except for the visual backbone with a learning rate of 10^{-5} . Beginning from the 40th epoch, we decrease the learning rate by a factor of 10. The window length K for temporal reasoning is set to 5. We conduct end-to-end training on 6 NVIDIA RTX A6000 GPUs, with a batch size of 6. During inference, the model operates without the need for post-processing, such as non-maximum suppression [8]. We employ detection thresholds $\beta_{obj} = 0.7$ and a referring threshold $\beta_{ref} = 0.3$ to localize visible objects and filter referent targets.

4.2. Qualitative Results

We visualize some examples in Fig. 6. In each referring example, the upper panels visualize the predicted tracked referent targets by TellTrack, and the lower panels show all detected visible objects by TellTrack. As depicted, our method can identify and track the referent targets accurately, even in various challenging situations, such as multiple objects, change of object status, and varying number of instances. TellTrack can precisely understand and recognize the meaning of object category, color, and position intentions in the text prompts. Consider the above panels of each example. In Fig. 6 (a), TellTrack successfully identifies the concepts “vehicles with light color”, and “opposite direction”. In Fig. 6 (b), the model understands the meaning of “red” and “ahead of us”, tracking the red car with ID 551, while filtering out the red car with ID 555 on the left. Similarly, the

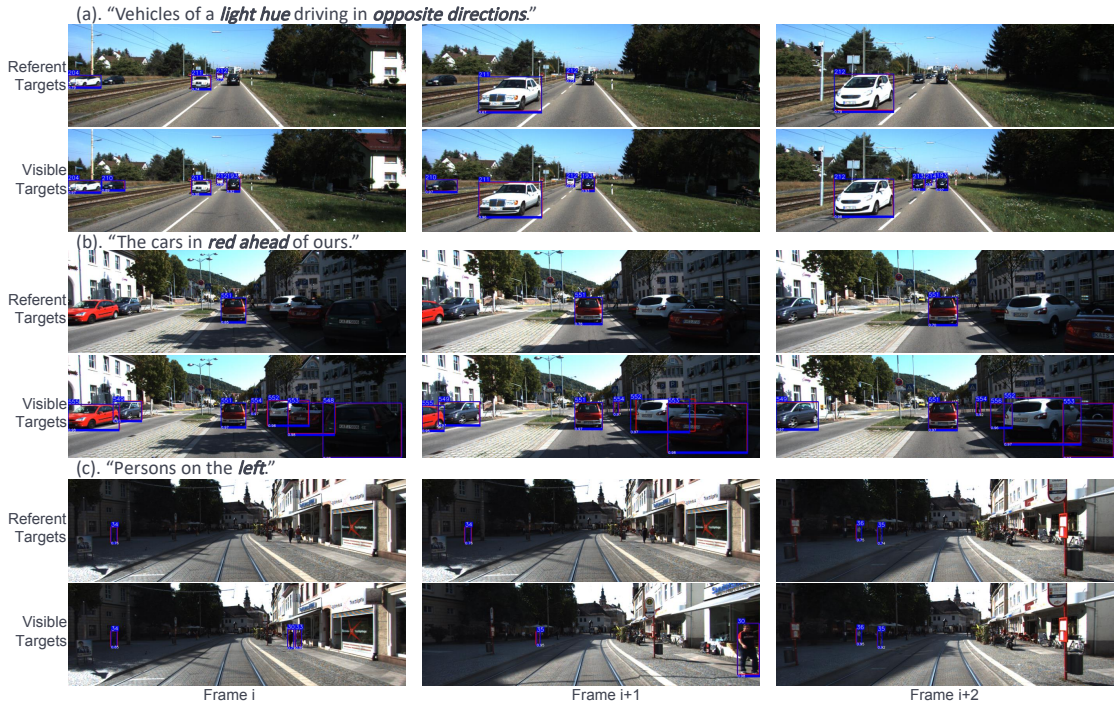


Figure 6. Qualitative examples. The above panels of each example visualize the predicted referent targets of TellTrack. The bottom panels show all visible objects detected by TellTrack. Blue bounding boxes stand for model predictions and the red bounding boxes are the ground truths. The number above each prediction is the assigned ID for that target, and the same ID across each frame represents the active tracking. The number below each prediction is the referring score/object score, respectively. Zoom in on the figures for more details.

Method	E ^a	Refer-KITTI								Refer-KITTI-V2							
		HOTA \uparrow	DetA \uparrow	AssA \uparrow	DetRe \uparrow	DetPr \uparrow	AssRe \uparrow	AssPr \uparrow	LocA \uparrow	HOTA \uparrow	DetA \uparrow	AssA \uparrow	DetRe \uparrow	DetPr \uparrow	AssRe \uparrow	AssPr \uparrow	LocA \uparrow
FairMOT [44]	✗	22.78	14.43	39.11	16.44	45.48	43.05	71.65	74.77	22.53	15.80	32.82	20.60	37.03	36.21	71.94	78.28
ByteTrack [45]	✗	24.95	15.50	43.11	18.25	43.48	48.64	70.72	73.90	24.59	16.78	36.63	22.60	36.18	41.00	69.63	78.00
iKUN [15]	✗	48.84	35.74	66.80	51.97	52.25	72.95	87.09	- ^b	10.32	2.17	49.77	2.36	19.75	58.48	68.64	74.56
TransRMOT [35]	✓	46.56	37.97	57.33	49.69	60.10	60.02	89.67	90.33	31.00	19.40	49.68	36.41	28.97	54.59	82.29	89.82
TempRMOT [47]	✓	52.21	40.95	66.75	55.65	59.25	71.82	87.76	90.40	35.04	22.97	53.58	34.23	40.41	59.50	81.29	90.07
Ours	✓	55.63	43.73	70.77	62.68	59.12	74.52	93.39	89.83	37.22	23.38	59.25	39.12	36.74	64.85	86.92	91.08

^a "E" means end-to-end training.

^b iKUN conducts oracle experiments, i.e., the bounding boxes are revised based on ground truth.

Table 1. Quantitative results of our method and the state-of-the-art baselines. The best performance is highlighted in red.

model successfully only tracks the people on the left while filtering out all people on the right. On the other hand, TellTrack maintains outstanding object detection performance, as illustrated in the bottom row of each example.

4.3. Quantitative Results

We examine the proposed method and several competitors in Tab. 1. For the "detect-and-track" methods, i.e., FairMOT[44], ByteTrack[45], we integrated the encoder into the detection module, followed by independent trackers to associate each referent target, for a fair comparison. iKUN [15] adopts the same paradigm exploiting a foundation model CLIP [30] to adaptively extract visual features. For the one-stage methods, we compare TellTrack with TransRMOT [35] and TempRMOT [47]. On both datasets, our method achieves a superior performance (HOTA of 55.63% on Refer-KITTI, and 37.22% on Refer-KITTI-V2). Specifically, we surpass the previous best

model, TempRMOT [47], by a significant margin of 2.18% on HOTA, and beats all other competitors in 7/8 metrics.

4.4. Ablation Study

To investigate the effect of core components in TellTrack, we conduct extensive ablation studies on Refer-KITTI-V2. Table 2 illustrates the results of all combinations of our proposed components. Every combination exhibits a positive impact on the overall performance. Specifically, using CME effectively fuses the information from different modalities, remarkably improving the association (+2.84% on AssA). This may be because the information exchange between the patches benefits the feature extraction of the objects spanning multiple patches. CQM, on the other hand, improves detection and association simultaneously, thanks to more activations for the detection queries during training. RIQA provides explicit intention guidance to the queries, boosting the reasoning ability of the model and, therefore, leading to

Components			Metrics							
RIQA	CQM	CME	HOTA \uparrow	DetA \uparrow	AssA \uparrow	DetRe \uparrow	DetPr \uparrow	AssRe \uparrow	AssPr \uparrow	LocA \uparrow
		✓	35.04	22.97	53.58	34.23	40.41	59.50	81.29	90.07
	✓		35.66	22.54	56.42	45.99	30.65	63.62	81.77	90.98
	✓	✓	36.06	23.05	56.43	39.20	35.87	61.80	85.92	91.08
		✓	36.27	23.16	56.80	41.02	34.73	63.52	81.67	91.58
✓			36.23	23.07	56.90	34.99	40.37	60.97	89.31	90.55
✓	✓		36.45	23.40	56.71	38.61	37.35	61.71	87.22	90.76
✓	✓	✓	36.77	23.96	56.41	42.38	35.54	61.83	86.16	90.20
✓	✓	✓	37.22	23.38	59.25	39.12	36.74	64.85	86.92	91.08

Table 2. Ablation studies of different components in TellTrack.

Method		Metrics							
1. Pre-decoder		HOTA \uparrow	DetA \uparrow	AssA \uparrow	DetRe \uparrow	DetPr \uparrow	AssRe \uparrow	AssPr \uparrow	LocA \uparrow
Q_{Detect}		35.45	22.77	55.19	50.08	29.46	62.65	80.80	85.14
	✓	35.88	23.73	54.26	51.78	30.46	61.59	80.32	82.58
✓	✓	36.23	23.07	56.90	34.99	40.37	60.97	89.31	90.55
2. In-decoder		35.05	22.60	54.37	35.86	37.94	59.99	84.27	89.06

Table 3. Effects of different RIQA. For pre-decoder adaptation, the sentence embedding can be infused with either detection queries, track queries, or both.

β_{ref}	HOTA	DetA	AssA	DetRe	DetPr	AssRe	AssPr	LocA
0.2	37.06	23.80	57.72	43.06	34.73	64.30	82.74	91.03
0.3	37.22	23.38	59.25	39.12	36.74	64.85	86.92	91.08
0.4	36.84	23.86	56.88	39.71	37.42	62.69	83.66	91.10
0.5	36.03	23.22	55.91	36.49	38.97	60.97	84.30	91.17
0.6	34.94	22.07	55.33	32.56	40.65	59.62	85.46	91.26
0.7	33.39	20.45	54.54	27.93	43.27	58.11	86.91	91.47
0.8	29.99	17.15	52.45	21.17	47.47	55.09	88.72	91.85

Table 4. Performance of the model on different β_{ref} .

a significant improvement in association (+3.32% on AssA, and +8.02% on AssPr).

We also investigate the effect of two types of RIQA, as shown in Tab. 3. For pre-decoder adaptation, we examine the effect of infusing sentence embedding with detection queries, track queries, and both. The results indicate that RIQA improves performance compared to decoding by vanilla queries. Surprisingly, we do not observe significant improvement in in-decoder adaptation compared with the baseline. We assume this is because the self-attention between the sentence embedding and the queries interferes with the semantic information of the queries, which impacts the performance. In addition, we investigate the effect of referring threshold β_{ref} in Tab. 4. In inference, depending on this threshold, the model predicts whether the detected object fits the referring text. Overall, β_{ref} has a significant impact on the balance between precision and recall. A lower threshold favors a better balance and, therefore, maximizes HOTA. When the threshold goes up, the model prioritizes precision at the cost of recall, reducing HOTA. TellTrack achieves the best performance when $\beta_{ref} = 0.3$.

Lastly, we examine the inference speed of TellTrack, crucial for real-world applications. While the baseline, TempRMOT, achieves 15.13 FPS, TellTrack maintains a comparable 15.08 FPS with improved performance.

5. Related Work

5.1. Referring Understanding

The core challenge of referring understanding is to model the semantic alignment of cross-modal sources. Early methods [10, 23, 27] mainly fuse the sources in two stages: 1). Adopting an off-the-shelf object detector to propose massive object proposals. 2). Leveraging a semantic alignment model to learn the similarity between proposals and language expression and find best-fitted objects. Nevertheless, the performance of these methods heavily relies on the quality of the object detector. Later approaches [5, 20] fuse multiple modalities on early features employing a cross-modal attention mechanism instead of proposals. Additionally, some works provide better semantic alignment interpretability via graph modeling [38], progressive reasoning [39], or multi-temporal-range learning [13].

5.2. Multi-Object Tracking

Prior works [2, 6, 11] adopt a two-stage *detect-and-track* paradigm. They first detect objects in each frame, and then associate the detections across frames, thereby tracking individual objects over time. Recent works [28, 43, 46] propose *one-stage* trackers, mostly based on trainable transformer [33] encoder-decoder architecture. They formulate MOT as a set prediction problem, by representing objects implicitly in the decoder queries, which are embeddings used by the decoder to output bounding box coordinates and class predictions. To further improve the performance, some efforts investigate the use of temporal memory [7], domain adaptation [40], and label reassignment [37, 41].

5.3. Referring Tracking

Referring SOT has been studied for several years. Most recent SOTA solutions mainly follow the joint tracking paradigm. MTTR [5] applies a DETR-like [9] multi-modal module to decode instance-level features into a set of multi-modal sequences. ReferFormer [36] inputs a set of object queries conditioned on language descriptions into Transformer to estimate the referred object. As for RMOT, Along with Refer-KITTI, the first baseline model TransRMOT [35] is introduced. It is built upon the end-to-end multi-object tracking method MOTR [43] to accept the cross-modal input. The latter approach, iKUN [15], follows a two-stage paradigm. It first explicitly extracts object proposals and then selects the objects matched with the language expression. On the other hand, it introduces a neural version of Kalman filter to dynamically adjust process noise and observation noise based on the current motion status. On top of TransRMOT, TempRMOT [47] integrates historical information into the model, refining the predictions with the help of the outputs from previous frames.

6. Conclusion

We present a novel end-to-end framework RMOT algorithm, TellTrack. We introduce a new matching strategy

during training, which effectively alleviates the imbalanced activations between detection queries and track queries caused by the difference in the number of newborn targets and existing targets in the dataset. We also propose a query adaptation component that explicitly fuses the linguistic intention with the decoder queries, and enhances the reasoning. Besides, we redesign the encoder to improve multi-modal fusion. TellTrack is evaluated on the widely used datasets and achieves the SOTA performance, demonstrating the effectiveness of our proposed components.

References

- [1] Rami Al-Rfou, Dokook Choe, Noah Constant, Mandy Guo, and Llion Jones. Character-level language modeling with deeper self-attention. In *Proceedings of the AAAI conference on artificial intelligence*, pages 3159–3166, 2019. 6
- [2] Philipp Bergmann, Tim Meinhardt, and Laura Leal-Taixé. Tracking without bells and whistles. In *Proceedings of the IEEE/CVF international conference on computer vision*, pages 941–951, 2019. 8
- [3] Luca Bertinetto, Jack Valmadre, Joao F Henriques, Andrea Vedaldi, and Philip HS Torr. Fully-convolutional siamese networks for object tracking. In *Computer Vision—ECCV 2016 Workshops: Amsterdam, The Netherlands, October 8–10 and 15–16, 2016, Proceedings, Part II 14*, pages 850–865. Springer, 2016. 1
- [4] David S Bolme, J Ross Beveridge, Bruce A Draper, and Yui Man Lui. Visual object tracking using adaptive correlation filters. In *2010 IEEE computer society conference on computer vision and pattern recognition*, pages 2544–2550. IEEE, 2010. 1
- [5] Adam Botach, Evgenii Zheltonozhskii, and Chaim Baskin. End-to-end referring video object segmentation with multi-modal transformers. In *Proceedings of the IEEE/CVF Conference on Computer Vision and Pattern Recognition*, pages 4985–4995, 2022. 8
- [6] Guillem Brasó and Laura Leal-Taixé. Learning a neural solver for multiple object tracking. In *Proceedings of the IEEE/CVF conference on computer vision and pattern recognition*, pages 6247–6257, 2020. 8
- [7] Jiarui Cai, Mingze Xu, Wei Li, Yuanjun Xiong, Wei Xia, Zhuowen Tu, and Stefano Soatto. Memot: Multi-object tracking with memory. In *Proceedings of the IEEE/CVF Conference on Computer Vision and Pattern Recognition*, pages 8090–8100, 2022. 8
- [8] John Canny. A computational approach to edge detection. *IEEE Transactions on pattern analysis and machine intelligence*, (6):679–698, 1986. 6
- [9] Nicolas Carion, Francisco Massa, Gabriel Synnaeve, Nicolas Usunier, Alexander Kirillov, and Sergey Zagoruyko. End-to-end object detection with transformers. In *European conference on computer vision*, pages 213–229. Springer, 2020. 5, 6, 8
- [10] Hanning Chen, Wenjun Huang, Yang Ni, Sanggeon Yun, Fei Wen, Hugo Latapie, and Mohsen Imani. Taskclip: Extend large vision-language model for task oriented object detection. *arXiv preprint arXiv:2403.08108*, 2024. 8
- [11] Patrick Dendorfer, Aljosa Osep, Anton Milan, Konrad Schindler, Daniel Cremers, Ian Reid, Stefan Roth, and Laura Leal-Taixé. Motchallenge: A benchmark for single-camera multiple target tracking. *International Journal of Computer Vision*, 129:845–881, 2021. 8
- [12] Thierry Deruyttere, Simon Vandenhende, Dusan Grujicic, Luc Van Gool, and Marie-Francine Moens. Talk2car: Taking control of your self-driving car. *arXiv preprint arXiv:1909.10838*, 2019. 1
- [13] Zihan Ding, Tianrui Hui, Junshi Huang, Xiaoming Wei, Jizhong Han, and Si Liu. Language-bridged spatial-temporal interaction for referring video object segmentation. In *Proceedings of the IEEE/CVF Conference on Computer Vision and Pattern Recognition*, pages 4964–4973, 2022. 8
- [14] Alexey Dosovitskiy, Lucas Beyer, Alexander Kolesnikov, Dirk Weissenborn, Xiaohua Zhai, Thomas Unterthiner, Mostafa Dehghani, Matthias Minderer, Georg Heigold, Sylvain Gelly, et al. An image is worth 16x16 words: Transformers for image recognition at scale. *arXiv preprint arXiv:2010.11929*, 2020. 5
- [15] Yunhao Du, Cheng Lei, Zhicheng Zhao, and Fei Su. ikun: Speak to trackers without retraining. In *Proceedings of the IEEE/CVF Conference on Computer Vision and Pattern Recognition*, pages 19135–19144, 2024. 7, 8
- [16] Heng Fan, Liting Lin, Fan Yang, Peng Chu, Ge Deng, Sijia Yu, Hexin Bai, Yong Xu, Chunyuan Liao, and Haibin Ling. Lasot: A high-quality benchmark for large-scale single object tracking. In *Proceedings of the IEEE/CVF conference on computer vision and pattern recognition*, pages 5374–5383, 2019. 1
- [17] Menglin Jia, Luming Tang, Bor-Chun Chen, Claire Cardie, Serge Belongie, Bharath Hariharan, and Ser-Nam Lim. Visual prompt tuning. In *European conference on computer vision*, pages 709–727. Springer, 2022. 5
- [18] Anna Khoreva, Anna Rohrbach, and Bernt Schiele. Video object segmentation with language referring expressions. In *Computer Vision—ACCV 2018: 14th Asian Conference on Computer Vision, Perth, Australia, December 2–6, 2018, Revised Selected Papers, Part IV 14*, pages 123–141. Springer, 2019. 1
- [19] Alexander Kirillov, Eric Mintun, Nikhila Ravi, Hanzi Mao, Chloe Rolland, Laura Gustafson, Tete Xiao, Spencer Whitehead, Alexander C Berg, Wan-Yen Lo, et al. Segment anything. In *Proceedings of the IEEE/CVF International Conference on Computer Vision*, pages 4015–4026, 2023. 2, 4
- [20] Muchen Li and Leonid Sigal. Referring transformer: A one-step approach to multi-task visual grounding. *Advances in neural information processing systems*, 34:19652–19664, 2021. 8
- [21] Tsung-Yi Lin, Michael Maire, Serge Belongie, James Hays, Pietro Perona, Deva Ramanan, Piotr Dollár, and C Lawrence Zitnick. Microsoft coco: Common objects in context. In *Computer Vision—ECCV 2014: 13th European Conference, Zurich, Switzerland, September 6–12, 2014, Proceedings, Part V 13*, pages 740–755. Springer, 2014. 6

- [22] Tsung-Yi Lin, Priya Goyal, Ross Girshick, Kaiming He, and Piotr Dollár. Focal loss for dense object detection. In *Proceedings of the IEEE international conference on computer vision*, pages 2980–2988, 2017. 6
- [23] Daqing Liu, Hanwang Zhang, Feng Wu, and Zheng-Jun Zha. Learning to assemble neural module tree networks for visual grounding. In *Proceedings of the IEEE/CVF International Conference on Computer Vision*, pages 4673–4682, 2019. 8
- [24] Shilong Liu, Feng Li, Hao Zhang, Xiao Yang, Xianbiao Qi, Hang Su, Jun Zhu, and Lei Zhang. Dab-detr: Dynamic anchor boxes are better queries for detr. *arXiv preprint arXiv:2201.12329*, 2022. 4
- [25] Jonathon Luiten, Aljosa Osep, Patrick Dendorfer, Philip Torr, Andreas Geiger, Laura Leal-Taixé, and Bastian Leibe. Hota: A higher order metric for evaluating multi-object tracking. *International journal of computer vision*, 129:548–578, 2021. 6
- [26] Chenxu Luo, Xiaodong Yang, and Alan Yuille. Exploring simple 3d multi-object tracking for autonomous driving. In *Proceedings of the IEEE/CVF international conference on computer vision*, pages 10488–10497, 2021. 1
- [27] Junhua Mao, Jonathan Huang, Alexander Toshev, Oana Camburu, Alan L Yuille, and Kevin Murphy. Generation and comprehension of unambiguous object descriptions. In *Proceedings of the IEEE conference on computer vision and pattern recognition*, pages 11–20, 2016. 8
- [28] Tim Meinhardt, Alexander Kirillov, Laura Leal-Taixe, and Christoph Feichtenhofer. Trackformer: Multi-object tracking with transformers. In *Proceedings of the IEEE/CVF conference on computer vision and pattern recognition*, pages 8844–8854, 2022. 8
- [29] Depu Meng, Xiaokang Chen, Zejia Fan, Gang Zeng, Houqiang Li, Yuhui Yuan, Lei Sun, and Jingdong Wang. Conditional detr for fast training convergence. In *Proceedings of the IEEE/CVF international conference on computer vision*, pages 3651–3660, 2021. 4
- [30] Alec Radford, Jong Wook Kim, Chris Hallacy, Aditya Ramesh, Gabriel Goh, Sandhini Agarwal, Girish Sastry, Amanda Askell, Pamela Mishkin, Jack Clark, et al. Learning transferable visual models from natural language supervision. In *International conference on machine learning*, pages 8748–8763. PMLR, 2021. 7
- [31] Nikhila Ravi, Valentin Gabeur, Yuan-Ting Hu, Ronghang Hu, Chaitanya Ryali, Tengyu Ma, Haitham Khedr, Roman Rädle, Chloe Rolland, Laura Gustafson, et al. Sam 2: Segment anything in images and videos. *arXiv preprint arXiv:2408.00714*, 2024. 2
- [32] Hamid Rezatofighi, Nathan Tsoi, JunYoung Gwak, Amir Sadeghian, Ian Reid, and Silvio Savarese. Generalized intersection over union: A metric and a loss for bounding box regression. In *Proceedings of the IEEE/CVF conference on computer vision and pattern recognition*, pages 658–666, 2019. 6
- [33] A Vaswani. Attention is all you need. *Advances in Neural Information Processing Systems*, 2017. 8
- [34] Yingming Wang, Xiangyu Zhang, Tong Yang, and Jian Sun. Anchor detr: Query design for transformer-based detector. In *Proceedings of the AAAI conference on artificial intelligence*, pages 2567–2575, 2022. 4
- [35] Dongming Wu, Wencheng Han, Tiancai Wang, Xingping Dong, Xiangyu Zhang, and Jianbing Shen. Referring multi-object tracking. In *Proceedings of the IEEE/CVF conference on computer vision and pattern recognition*, pages 14633–14642, 2023. 1, 2, 4, 6, 7, 8
- [36] Jiannan Wu, Yi Jiang, Peize Sun, Zehuan Yuan, and Ping Luo. Language as queries for referring video object segmentation. In *Proceedings of the IEEE/CVF Conference on Computer Vision and Pattern Recognition*, pages 4974–4984, 2022. 8
- [37] Feng Yan, Weixin Luo, Yujie Zhong, Yiyang Gan, and Lin Ma. Bridging the gap between end-to-end and non-end-to-end multi-object tracking. *arXiv preprint arXiv:2305.12724*, 2023. 8
- [38] Sibe Yang, Guanbin Li, and Yizhou Yu. Cross-modal relationship inference for grounding referring expressions. In *Proceedings of the IEEE/CVF conference on computer vision and pattern recognition*, pages 4145–4154, 2019. 8
- [39] Sibe Yang, Meng Xia, Guanbin Li, Hong-Yu Zhou, and Yizhou Yu. Bottom-up shift and reasoning for referring image segmentation. In *Proceedings of the IEEE/CVF Conference on Computer Vision and Pattern Recognition*, pages 11266–11275, 2021. 8
- [40] En Yu, Songtao Liu, Zhuoling Li, Jinrong Yang, Zeming Li, Shoudong Han, and Wenbing Tao. Generalizing multiple object tracking to unseen domains by introducing natural language representation. In *Proceedings of the AAAI Conference on Artificial Intelligence*, pages 3304–3312, 2023. 8
- [41] En Yu, Tiancai Wang, Zhuoling Li, Yuang Zhang, Xiangyu Zhang, and Wenbing Tao. Motrv3: Release-fetch supervision for end-to-end multi-object tracking. *arXiv preprint arXiv:2305.14298*, 2023. 8
- [42] Licheng Yu, Patrick Poirson, Shan Yang, Alexander C Berg, and Tamara L Berg. Modeling context in referring expressions. In *Computer Vision—ECCV 2016: 14th European Conference, Amsterdam, The Netherlands, October 11–14, 2016, Proceedings, Part II 14*, pages 69–85. Springer, 2016. 1
- [43] Fangao Zeng, Bin Dong, Yuang Zhang, Tiancai Wang, Xiangyu Zhang, and Yichen Wei. Motr: End-to-end multiple-object tracking with transformer. In *European Conference on Computer Vision*, pages 659–675. Springer, 2022. 2, 8
- [44] Yifu Zhang, Chunyu Wang, Xinggang Wang, Wenjun Zeng, and Wenyu Liu. Fairmot: On the fairness of detection and re-identification in multiple object tracking. *International journal of computer vision*, 129:3069–3087, 2021. 7
- [45] Yifu Zhang, Peize Sun, Yi Jiang, Dongdong Yu, Fucheng Weng, Zehuan Yuan, Ping Luo, Wenyu Liu, and Xinggang Wang. Bytetrack: Multi-object tracking by associating every detection box. In *European conference on computer vision*, pages 1–21. Springer, 2022. 7
- [46] Yuang Zhang, Tiancai Wang, and Xiangyu Zhang. Motrv2: Bootstrapping end-to-end multi-object tracking by pre-trained object detectors. In *Proceedings of the IEEE/CVF Conference on Computer Vision and Pattern Recognition*, pages 22056–22065, 2023. 8

- [47] Yani Zhang, Dongming Wu, Wencheng Han, and Xingping Dong. Bootstrapping referring multi-object tracking. *arXiv preprint arXiv:2406.05039*, 2024. [2](#), [4](#), [6](#), [7](#), [8](#)
- [48] Xizhou Zhu, Weijie Su, Lewei Lu, Bin Li, Xiaogang Wang, and Jifeng Dai. Deformable detr: Deformable transformers for end-to-end object detection. *arXiv preprint arXiv:2010.04159*, 2020. [2](#), [4](#), [5](#), [6](#)